Diffusion Tensor Imaging of Rostral Brain Areas in Patients with Congenital Central Hypoventilation Syndrome

R. Kumar[1], P. M. Macey[2,3], M. A. Woo[2], and R. M. Harper[1,3]
[1]Neurobiology, David Geffen School of Medicine at UCLA, Los Angeles, CA, United States, [2]School of Nursing, UCLA, Los Angeles, CA, United States, [3]Brain Research Institute, UCLA, Los Angeles, CA, United States

Introduction:

Congenital central hypoventilation syndrome (CCHS) is associated with mutations of the PHOX2B gene, and patients show a range of abnormal physiologic and autonomic alterations. Physiologic characteristics include insensitivity to CO_2 and O_2, reduced drive to breathe during sleep, and autonomic deficits, including exaggerated sweating, abnormal heart rate variability, loss of nocturnal "dipping" in blood pressure, abnormal pupillary dilation, and poor temperature control. In addition, CCHS patients show cognitive and affective impairments. The autonomic and behavioral deficits suggest both caudal and rostral brain injuries, which may result from maldevelopment of brain structures affected with PHOX2B mutations in early life, or from multiple hypoxic episodes resulting from the primary breathing condition. Brain structural deficits appear in multiple regions, based on T2-relaxometry and mean diffusivity procedures (1, 2). Several pathological conditions could produce these findings; however, both T2-relaxometry and mean diffusivity measures indicate generalized tissue damage, but do not differentiate types of axonal injury. Axial diffusivity measures diffusion of water molecules parallel to axons, and indicates axonal status, and radial diffusivity measures diffusion of water perpendicular to fibers, and shows myelin changes. Caudal brain sites, including brainstem and cerebellar regions have been evaluated in CCHS for extent and different types of tissue injury (3); however, rostral brain areas have not been evaluated. Assessment of axial and radial diffusivity in rostral brain regions may provide more insights into the different types of tissue injury in CCHS. The aim was to assess axial and radial diffusivity in rostral brain areas in CCHS to detect different types of axonal tissue injuries present in the syndrome.

Materials and methods:

Twelve CCHS (mean age ± SD: 18.5 ± 4.9 years; 7 male) and 30 control (17.7 ± 4.6 years; 18 male) subjects were studied. CCHS diagnosis was made based on standard criteria, and only those subjects requiring ventilatory support during sleep were recruited from CCHS family network (http://cchsnetwork.org). CCHS subjects with additional conditions, such as cardiovascular or neurological disorders, or Hirschsprung's disease, were excluded. All control subjects were healthy, and were recruited from the university campus community. Brain MRI studies were performed using a 3.0-Tesla MRI scanner (Magnetom Tim-Trio; Siemens), with an 8-channel phased-array heal-coil. Diffusion tensor imaging was performed in the axial plane, using a single-shot echo-planar-imaging with twice-refocused spin-echo pulse sequence (TR = 10,000 ms; TE = 87 ms; FA = 90°; BW = 1346 Hz/ pixel; matrix size = 128×128; FOV = 230×230 mm; thickness = 2.0 mm, no interslice gap; gradient directions = 64; b = 0 and 700 s/mm^2). The parallel imaging technique, GRAPPA, was used with an acceleration factor of two, and two DTI series were collected separately for subsequent averaging. Data were processed using the SPM8, DTI-Studio (v 3.0.1), and MATLAB-based custom software. Using b0 and diffusion-weighted images, diffusion tensor matrices were calculated and three principal eigenvalues (λ1, λ2, and λ3) were derived. Using principal eigenvalues, axial diffusivity ($\lambda_{\parallel} = \lambda 1$) and radial diffusivity [$\lambda_{\perp} = (\lambda 2+\lambda 3)/2$] maps were derived from each DTI series. For each subject, the two axial and two radial diffusivity maps derived from each DTI series were each realigned, and averaged to create one map of each type per subject. Axial and radial diffusivity maps were normalized to Montreal Neurological Institute space, and smoothed. The normalized and smoothed axial and radial diffusivity maps were compared voxel-by-voxel between groups using analysis of covariance (covariates: age and gender; threshold: $p<0.005$, uncorrected). A brain mask was used during group comparison to suppress regions showing damage in brainstem and cerebellar sites. Statistical parametric maps, indicating significant differences in axial and radial diffusivity between groups, were created for regions showing increased radial diffusivity only, increased axial diffusivity only, and both increased axial and radial diffusivity, and overlaid onto background images, created by averaging all normalized b0 images of CCHS and control subjects, for structural identification.

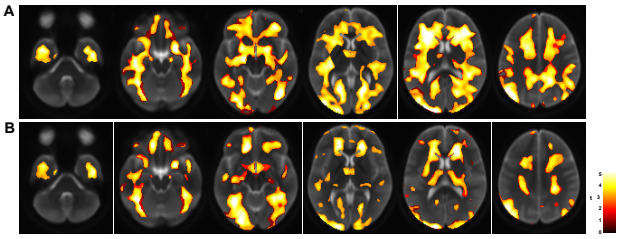

Fig.1: Brain sites showing increased Radial (A) and axial (B) diffusivity in CCHS over control subjects.

Results:

No significant differences in age, gender, or body-mass-index appeared between the groups. Radial (Fig. 1A) and axial (Fig. 1B) diffusivity were significantly increased in several rostral brain areas in CCHS over control subjects. No regions showed significantly higher axial or radial diffusivity in control over CCHS subjects.

Brain regions with significantly higher radial diffusivity in CCHS, without significant changes in axial diffusivity, emerged in the right prefrontal, bilateral parietal and medial occipital cortices, bilateral anterior, mid and posterior cingulate cortices extending to the cingulum bundle, bilateral corona radiata, corpus callosum, insular cortices, interior limb of internal capsules extending to the caudate nuclei, left anterior and posterior putamen, left posterior limb of internal capsule, bilateral ventrolateral temporal lobes, anterior hippocampus extending to amygdala, columns of the fornices, orbito-frontal cortices, and hypothalamus. Brain areas showed increased axial diffusivity only in bilateral radiata, cortico-pontine tracts, left frontal cortex and putamen, bilateral mid and posterior thalamus, posterior limb of internal capsules, orbito-frontal cortices, occipital lobes, right parietal cortices, bilateral ventrolateral temporal lobes, and right inferior fronto-occipital fasciculus. Both axial and radial diffusivity measures showed significantly higher values in bilateral corona radiata, left genu, anterior and mid cingulate cortices, and cingulum bundle, corpus callosum, right prefrontal cortex, anterior fornix bilaterally, hypothalamus extending to anterior and mid thalamus, orbito-frontal cortex and nearby white matter, anterior hippocampus extending to amygdala, caudate nuclei, right anterior and left mid/posterior insular cortices, putamen, ventral medial prefrontal cortex, parahippocampal gyrus, bilateral anterior limb of internal capsules, nucleus accumbens, inferior temporal lobes, temporo-occipital cortices, and inferior fronto-occipital fasciculus.

Discussion:

Extensive axonal injury appeared in the rostral brain; a significant proportion of major fiber systems was affected. Radial diffusivity, indicating myelin injury, appeared in the corona radiata, internal capsule, and corpus callosum. In addition, a major fiber system from the hippocampus through the fornix, as well as the cingulum bundle, and fibers within the temporal and parietal lobes also showed injury. Solely-axial diffusivity changes, suggesting axonal injury, appeared in the thalamus, internal capsule, corona radiata, and occipital and temporal lobes. Both axial and radial diffusivity changes, indicating loss of tissue integrity with both myelin and axonal injury, appeared in basal forebrain, limbic, occipital, and temporal areas. Several of these rostral areas show no Phox2b neuronal expression in murine models, suggesting that damage develops from processes other than direct action of mutations in PHOX2B. We speculate that areas of myelin deficits resulted from either maldevelopment or hypoxia, and regions with axonal deficits resulted from PHOX2B-related developmental issues. Other brain regions associated with myelin, together with axonal injury may develop from hypoxic episodes accompanying the syndrome.

References:

1. Kumar, R., Macey, P.M., Woo, M.A., Alger, J.R., Keens, T.G., Harper, R.M. *J. Comp. Neurol.* 487:361-371, 2005.
2. Kumar, R., Macey, P.M., Woo, M.A., Alger, J.R., Harper, R.M. *J. Magn. Reso. Imaging* 24: 1252-1258, 2006.
3. Kumar, R., Macey, P.M., Woo, M.A., Alger, J.R., Harper, R.M. *Pediatr. Res.* 64: 275-280, 2008.

Grants: Supported by HD- 22695.